Journal of Metals, Materials and Minerals, 35(3), e2336, 2025

Microwave absorption properties of porous activated carbon/nickel oxide composites derived from coconut husks

Mohamad Zul Aqiman SHUKERI[1], Nor Zakiah YAHAYA[1,*], Ezzan Afifah ZAINUDDIN[1], Nazri MAHMUD[2], Liyana ZAHID[3] and Hasliza A RAHIM[3,4]

[1] *Physics Section, School of Distance Education, Universiti Sains Malaysia, Pulau Pinang 11800, Malaysia*
[2] *School of Electrical and Electronic Engineering, Universiti Sains Malaysia, Engineering Campus Seberang Perai Selatan, Nibong Tebal, Penang 14300 Malaysia*
[3] *Centre of Excellence for Advanced Communication Engineering (ACE), Universiti Malaysia Perlis (UniMAP), 01000 Kangar, Perlis, Malaysia*
[4] *Faculty of Electronic Engineering & Technology Universiti Malaysia Perlis (UniMAP), 02600 Arau, Perlis, Malaysia*

***Corresponding author e-mail**: norzakiah@usm.my

Received date:
25 February 2025
Revised date:
11 June 2025
Accepted date:
5 August 2025

Keywords:
Activated carbon;
Coconut husk;
MW absorber;
Porous structure;
Polymer composite

Abstract

Porous Activated Carbon (AC) is a promising material for microwave absorbing materials, showing potential in communication and modern warfare. The study explores the process of creating porous AC from coconut husks using hydrochloric acid and carbonization at varying temperatures, followed by doping AC with nickel oxide to create an AC/NiO polymer composite with varying thicknesses. These composites are compared to AC composites loaded in a paraffin matrix. The dielectric and microwave (MW) properties of the AC/NiO and AC polymer composites at various thicknesses were analyzed using a Performance (PNA)-X Network Analyzer. The study also examines the carbon content and porosity effect of the samples using Field Emission Scanning Electron Microscope (FESEM). The results show that the pore sizes and surface areas of the AC/NiO composites are larger than those of the AC composites. The presence of NiO enhances the dielectric and MW properties of the samples. AC and AC/NiO materials exhibit exceptional absorption more than 96%. However, AC/NiO composite carbonized at 350°C with a thickness of 6.0 mm exhibits excellent MW absorption performance, with a minimum RL peak value of –15 dB at 6.4 GHz. Overall, this study demonstrates the great potential of a polymer composite made from coconut husk-derived AC and NiO for MW absorption.

1. Introduction

In recent years, significant advancements in technology, particularly in electronics and wireless devices, have led to their widespread use across various fields. Microwave absorbing materials (MAMs) play a crucial role in protecting human and environmental health by managing and reducing electromagnetic pollution [1,2]. The growth of wireless communication technologies operating in the microwave frequency range has resulted in a continuous increase in electromagnetic (EM) pollution, raising serious global concerns [3,4]. The extensive emission of electromagnetic waves into the environment poses risks to public health and remains a primary focus for national defence and security. As a result, MAM technology has garnered increasing attention due to its diverse applications in both civilian and military sectors.

To address this issue, it is essential to develop and implement effective MAMs that can absorb and diminish unwanted electromagnetic radiation [5-7], thereby mitigating EM pollution. The primary goal is to create MAMs with high absorption efficiency across a wide frequency spectrum while ensuring they are lightweight, cost-effective, and environmentally sustainable. Utilizing sustainable sources for MAMs, such as carbon derived from agricultural waste, offers an eco-friendly alternative. Carbon derived from agricultural waste has emerged as a promising absorbing material due to its repeatability, environmental benefits, and natural abundance [8-10]. Additionally, carbon from biomass is lightweight, has favourable pore dimensions and conductive structures [11,12], and can be easily processed to enable rapid attenuation of electromagnetic waves, making it suitable to produce electromagnetic and electrical devices. Agricultural byproducts like rice husks [13,14], and banana peels [5,15] show significant potential as raw materials for fabricating microwave absorbers. These materials can be engineered to possess strong electrical conductivity, appropriate pore sizes, and low density [12-14] with all essential characteristics for effective absorption of electromagnetic waves.

The presence of porosity within the material enables electromagnetic wave dispersion and multiple reflections, expanding available wave propagation pathways [16]. Structures that are porous or hollow have a lower density and at the same time enhance the interactions that occur between EM waves and materials that absorb electromagnetic radiation. Recent studies have shown that the presence of a porous structure can significantly reduce the strength of EM waves [17,18]. The presence of pores expands material surface area, enabling multiple reflections and wave dispersion within the pores' walls. A longer travel length of electromagnetic waves, due to repeated reflections, increases the probability of wave absorption and subsequent decay [19]. Additionally,

AC can have different types of pores based on their sizes, such as ultra micropores (< 0.7 nm), supermicropores (0.7 nm to 2.0 nm), small mesopores (2.0 nm to 2.5 nm), and large mesopores (2.5 nm to 50 nm) [20]. Pore types depend on activating agents and activation temperature.

The selection of AC generated from coconut fibre as a constituent of MW absorbers is attributed to its distinctive porous carbon structure, which significantly contributes to impedance matching, interface polarisation, and the occurrence of multiple reflection and scattering losses [21,22]. The determination of AC quality relies on crucial parameters such as activation temperature and chemical-to-carbon impregnation ratio. The utilisation of coconut fibre has been proposed for the synthesis of AC. Currently, there is a lack of detailed studies specifying the synthesis conditions such as temperature and acid concentration needed to produce high performance activated carbon from coconut husks. This highlights the need to identify the optimal parameters for producing activated carbon with enhanced adsorptive properties.

For improved impedance matching and high-performance MW absorbing materials, the combination of carbon materials with magnetic materials is crucial. MOF-derived MAMs maintain their original porous framework and uniform pore distribution, enhancing magnetic properties. In this study, Nickel oxide (NiO) has been selected due to its affordability, malleability, minimal dielectric loss, and expansive surface area [23]. NiO has gained significant attention for its absorption intensity and frequency bandwidth characteristics [24] and is considered promising in energy storage and MW absorption domains [25].

2. Experimental details

2.1 Materials

Coconut husks were sourced from a local market near to Universiti Sains Malaysia in Pulau Pinang, Malaysia. For this study, only analytical grade chemical reagents were utilized, specifically 37% hydrochloric acid (diluted to a concentration of 1.0 M) and nickel(II) nitrate hexahydrate (99.0%), both procured from Chemist Chemicals in Malaysia.

2.2 Synthesis and characterization of materials

Figure 1 shows coconut fibre was obtained from coconut waste. The samples were washed with distilled water and then dried at 110°C for 24 h. The coconut shells were first dried before being carbonised in a furnace at 200°C for 1 h. After carbonisation, chemical activation was carried out using a 1 M HCl solution to improve porosity. All samples were immersed in a 1.0 M hydrochloric acid (HCl) solution at a 1:1 ratio for 24 h. The activated carbon (AC) samples were then filtered and rinsed with distilled water until a neutral pH was achieved, using filter paper. To reach the activation temperature, the material underwent thermal treatment at 110°C for 24 h. The samples were subsequently processed at temperatures of 250°C, 300°C, and 350°C, resulting in materials designated as AC 200, AC 250, AC 300, and AC 350. The composite AC/NiO was synthesised using a modified thermal co-precipitation method. Initially, 6.0 g of AC 200 was dispersed in 150 mL of deionised water with the assistance of a sonicator.

Figure 1. Schematic illustrations show the process from coconut fiber to composite material.

Subsequently, a 50 mL solution containing 8.815 g of $Ni(NO_3)_2{\cdot}6H_2O$ precursor was added to the dispersion and stirred for 2 h, while maintaining the pH of the mixture between 8 and 9. The mixture was then heated to 90°C for 6 h under continuous stirring. The resultant precipitate was subjected to filtration, washing, and drying at 110°C overnight. Finally, the product underwent calcination at a temperature of 250°C for 4 h to obtain the desired adsorbent materials. The sample is designated as AC/NiO 200. Additional samples were processed using AC 250, AC 300, and AC 350, and are designated as AC/NiO 250, AC/NiO 300, and AC/NiO 350, respectively. The prepared samples were combined with an epoxy resin at a weight ratio of 1:2 for dried for 24 h.

The morphological features were analyzed using a Field Emission Scanning Electron Microscope (FESEM, Hitachi S4800), which provides high-resolution surface imaging. Elemental composition was determined via Energy Dispersive X-ray Spectroscopy (EDX) integrated with the same FESEM system.

2.3 Measurement of dielectric properties and microwave properties

Microwave and dielectric properties were measured using an Agilent 8357B Vector Network Analyzer (VNA) over the 8 GHz to 12 GHz frequency range (X-band). The MW absorption properties of the samples were measured at thicknesses of 1 mm, 4 mm, and 6 mm. To evaluate the microwave absorption performance of materials as shown in Equation (5), the dielectric properties specified in Equation (1) are essential parameters.

$$\left(\varepsilon^* = \varepsilon' - \acute{\varepsilon}\right) \tag{1}$$

The real parts dielectric $\acute{\varepsilon}$ are associated with the storage capacity of EM wave energy, while the imaginary parts, $\acute{\varepsilon}$ indicate the loss capacity of EM wave energy [30]. Based on dielectric constants, the reflection loss (RL), which indicates a material's ability to absorb EM waves, can be calculated using transmission line theory [26-28], as demonstrated in the following Equation (4-5).

The quantification of the absorption efficiency of AC/NiO composites can be accurately achieved by utilizing the parameter of minimal reflection loss (RL_{min}) which is less than –10 dB indicates that 90% of the input electromagnetic waves are absorbed upon entering the material. This frequency range is referred to as the effective absorption band (EAB). Equation (2) provides a description of RL_{min}

utilising the transmission line methodology [29]. The transmission line theory was utilized in conjunction with the simulated reflection loss to carry out the procedure necessary for the calculation of the absorption loss, which are more often referred to as RL [30]. The reflection loss of the incident electromagnetic wave from the absorber can be considered insignificant due to Equation (5).

$$\mathrm{RL} = 20\, log_{10} \left| \frac{Z_{\mathrm{in}} + Z_{\mathrm{O}}}{Z_{\mathrm{in}} - Z_{\mathrm{O}}} \right| \tag{2}$$

$$Z_{\mathrm{in}} = Z_{\mathrm{O}} \sqrt{\frac{\mu_{\mathrm{r}}}{\varepsilon_{\mathrm{r}}}}\, tanh\left(\mathrm{j} \left(\frac{2\pi f d}{c} \right) \sqrt{\mu_{\mathrm{r}} \varepsilon_{\mathrm{r}}} \right) \tag{3}$$

RL is significantly controlled by impedance. Where Z_0 is the free space impedance, f represents the MW frequency, ε_r denotes the relative dielectric, μ_r denotes the complex permeability, d symbolizes the absorber thickness, c represents the velocity of EM wave propagation in vacuum, Z_{in} indicates absorbers impedance and represents the reflection loss. Formally, S11 is the negative of return loss and has a negative dB value:

$$S_{11} = -\,\mathrm{RL} = 20\ \log(|\Gamma|) \tag{4}$$

Absorptions equations are denoted by formula as follows:

$$\mathrm{A} = 1 - |S_{11}|^2 \tag{5}$$

3. Results and discussions

3.1 Effect of carbonization temperatures on structural of acs

Figure 2 illustrates the surface morphology of AC (Figure 2(a–d)) and AC/NiO (Figure 2(e–h)) at different carbonization temperatures under optimal conditions (1 h activation time and 1:1, HCl:AC impregnation ratio), characterized by a diameter ranging from 30 nm to 50 nm. As expected, AC at lower carbonization temperatures (200°C and 250°C) exhibits a nonporous surface, as depicted in Figure 2(a–b). Conversely, the surface of AC/NiO displays large and well developed pores, as shown in Figure 2(e–h), which can be attributed to the two steps activation process utilized. The impact of the activation temperature extends beyond the surface morphology to include the development of internal pore networks, with smaller pores preserved at lower temperatures and larger pores forming at higher temperatures.

Thermal treatment improves the pore structure of AC, leading to enhanced efficiency in MW absorbers by increasing the available surface area and facilitating multiple reflections and scattering of incident EM waves. MW-assisted activation creates a mesoporous structure, which further enhances the material's interaction with MW energy. Research indicates that the porosity effect on AC/NiO outperforms that of AC alone across all carbonization temperatures. Since the introduction emphasizes the importance of porous or hollow structures in reducing density and improving interactions with electromagnetic waves, a detailed quantitative analysis of pore size distribution and surface characteristics is crucial to validate these findings. This analysis will clarify the relationship between the materials' morphological evolution and their performance as EM wave absorbers. Our future work will include BET analysis to quantitatively confirm porosity and incorporate this characterization.

As the temperature for carbonization increases, so does the carbon content (Table 1). Several factors contribute to this trend. Firstly, higher temperatures facilitate the decomposition of organic materials, causing organic compounds to break down into carbon and release volatile substances. Secondly, as the carbonization temperature rises, there is a greater loss of non-carbon elements, especially oxygen, resulting in a material that is richer in carbon. The transition from AC 200 to AC 250 shows a significant increase in carbon content (approximately 4.14%), while the increase from AC 250 to AC 300 is minimal (0.07%). This suggests that further increases in temperature may yield diminishing returns in terms of carbon content. However, the substantial increase observed in AC 350 (5.75% higher than AC 300) suggests that there may be another phase of significant structural change or removal of remaining volatile substances. This can be attributed to the decomposition and reaction of siliceous impurities present in the precursor materials at elevated temperatures 300°C and 350°C. The significant increase from 0.26% to 1.74% indicates that beyond a certain temperature, the silica content becomes more prominent in the residue. This shift from predominantly AC to a material with substantial silica content can pose challenges for applications that require high-purity AC. High silica content can alter the material's physical and chemical properties, such as surface area, porosity, and adsorption capacity, as depicted in Figure 2(c,d,H).

When comparing the carbon content of the AC samples (64.69%, 68.83%, 68.90%, and 74.65%) with that of the AC/NiO samples, it can be observed that AC/NiO 200, AC/NiO 250, and AC/NiO 300 show a slight increase in carbon content compared to their pure AC counterparts. However, AC/NiO 350 exhibits a decrease in carbon content compared to AC 350. The addition of NiO may play a role in stabilizing the carbon structure or facilitating certain chemical reactions that result in a slight increase in carbon content at lower temperatures (200°C to 300°C). This could be attributed to interactions between NiO and the carbon matrix, potentially promoting further decomposition of non-carbon elements [22]. The decrease in carbon content at the highest temperature (AC/NiO 350) compared to AC 350 suggests that the presence of NiO might catalyze the combustion or oxidation of carbon, reducing its overall percentage. Additionally, NiO might affect the carbonization process at higher temperatures, leading to a different carbon yield. This is favourable for the enhanced magneticity and dielectric properties. The presence of C, O, Si and Ni in the composite is confirmed using EDX-mapping (Figure 3) and elemental composition analysis (Table 1).

3.2 Dielectric properties of AC and AC/NiO composites

To determine the MW absorption potential of the composites, the dielectric properties (ε' and ε'') of AC/NiO and AC composites with different temperature of carbonization were measured at X-band (8 GHz to 12 GHz) (Figure 4). Dielectric properties quantify the extent to which a material influences the electric field during its interaction with electromagnetic waves.

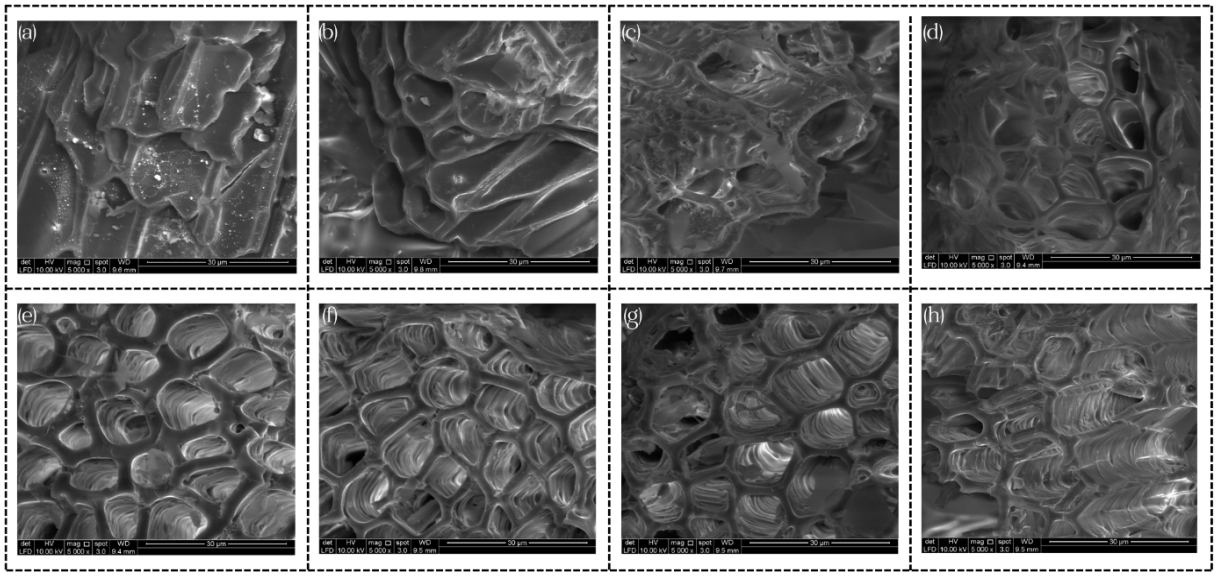

Figure 2. SEM images of (a) AC 200 (b) AC 250 (c) AC 300 (d) AC 350 (e) AC/NiO 200 (f) AC/NiO 250 (g) AC/NiO 300 (h) AC/NiO 350.

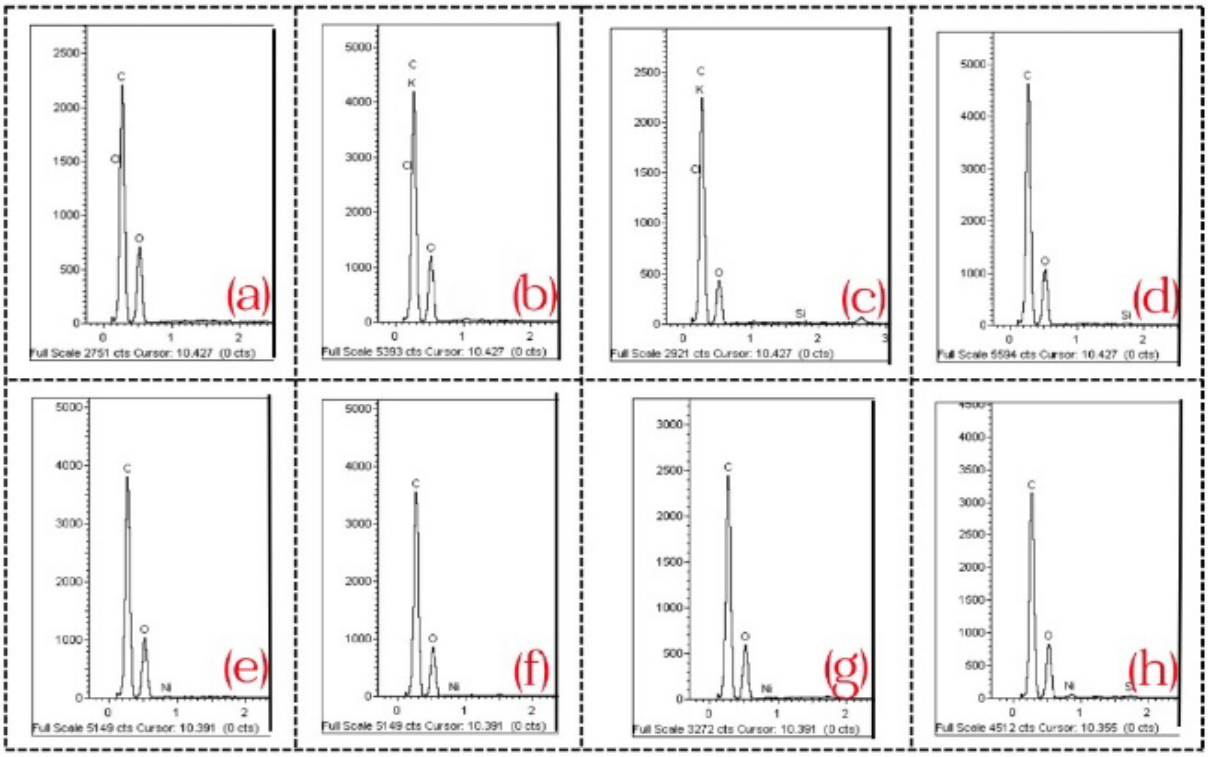

Figure 3. EDX mapping of (a) AC 200 (b) AC 250 (c) AC 300 (d) AC 350 (e) AC/NiO 200 (f) AC/NiO 250 (g) AC/NiO 300 (h) AC/NiO 350.

Table 1. Elemental compositions of AC and AC/NiO at various carbonization temperatures.

Sample	Weights percentage of the element [%]			
	C	O	Si	Ni
AC 200	64.69	35.31		
AC 250	68.83	31.17		
AC 300	68.90	30.84	0.26	
AC 350	74.65	23.61	1.74	
AC/NiO 200	66.30	32.93		0.77
AC/NiO 250	67.89	31.42		0.69
AC/NiO 300	68.51	31.17		0.32
AC/NiO 350	66.6	30.97	0.33	2.1

The curves of ε' and ε'' show a slightly decreasing trend in the frequency range from 8 GHz to 12 GHz. This is related to dipole polarization. The dielectric properties properties, ε' and ε" values increase with the carbonization temperatures for AC and AC/NiO samples, respectively. Increases the values of ε' and ε'' by introducing more defects and dipoles. The addition of NiO contributes of ε' values shift to the higher values (2.3 to 3.3) compared to AC alone (0.3 to 1.8) as shown in Figure 4(a-b). This is due to increased polarization and a more homogeneous distribution of nickel oxide within the carbon matrix (Figure (4(b)). The microstructure of the material may be particularly favourable for energy storage, as it has a high surface area and porous structure, contributing to a high dielectric constant due to the large number of charge storage sites. It is observed that the sample AC/NiO 350 possess the highest ε' and ε'' values which due the highest of carbon content and better porosity effect obtained in Table 1. Nickel oxide (NiO) is integral to various magnetic loss mechanisms, including ferromagnetic resonance and eddy current loss. When coupled with the dielectric loss inherent in the porous carbon structure, these mechanisms contribute to an enhanced effective microwave absorption. The flower-like morphology of NiO exhibits superior microwave absorption capabilities, attributable to its porous architecture, substantial surface area, effective impedance matching, and heightened dielectric loss resulting from interfacial polarization at the heterojunction [32,33].

However, the lowest ε' and ε'' values is obtained by AC 200, due to its nonporous structure and lowest carbon content. Meanwhile, the value dielectric properties of AC 250 to AC 300 are only slightly different, possibly due to minimal differences in carbon content (0.07%). The carbon matrix retains significant functional groups that contribute to polarization at 350°C. The increasing presence of silica not significantly affects the dielectric properties of the samples which silica content in AC 300 and AC 350 are only 0.26% and 1.74%, respectively.

3.3 MW absorption properties of AC and AC/NiO composites

Reflection loss, RL of AC and AC/NiO satisfied the of 90% value of absorption is achieved as shown in Figure 5. Resonant frequencies of samples of AC shifted to higher frequencies from 9.13 GHz to 9.4 GHz. When added the NiO, the resonant frequency shifted about 0.31 GHz for each sample of variant carbonization temperatures. However, the lowest S_{11} obtained by AC/NiO (–15.03 dB) followed by AC 350 (–14.72 dB) indicating a greater absorption efficiency at the corresponding frequency. This is due to NiO can also affect the resonant frequencies of samples. It has the potential to alter the absorption peaks and shift them to various frequencies, hence enabling the customization of absorption features.

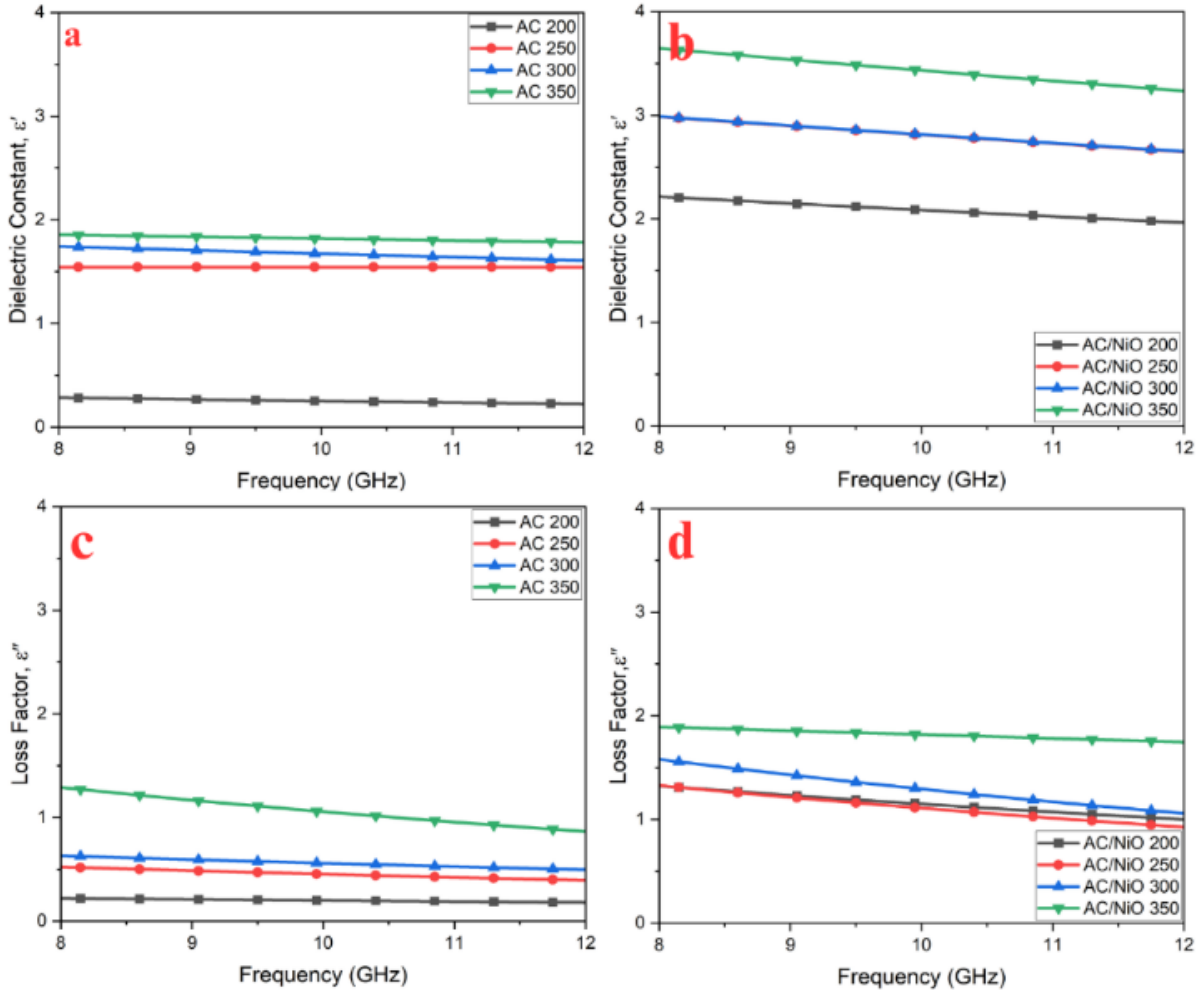

Figure 4. (a) Dielectric constant of AC, ε', (b) Dielectric constant of AC/NiO, ε' and (c) Loss Factor of AC, ε'' and (d) Loss Factor of AC/NiO, ε'' at X-band frequencies for different carbonization temperature.

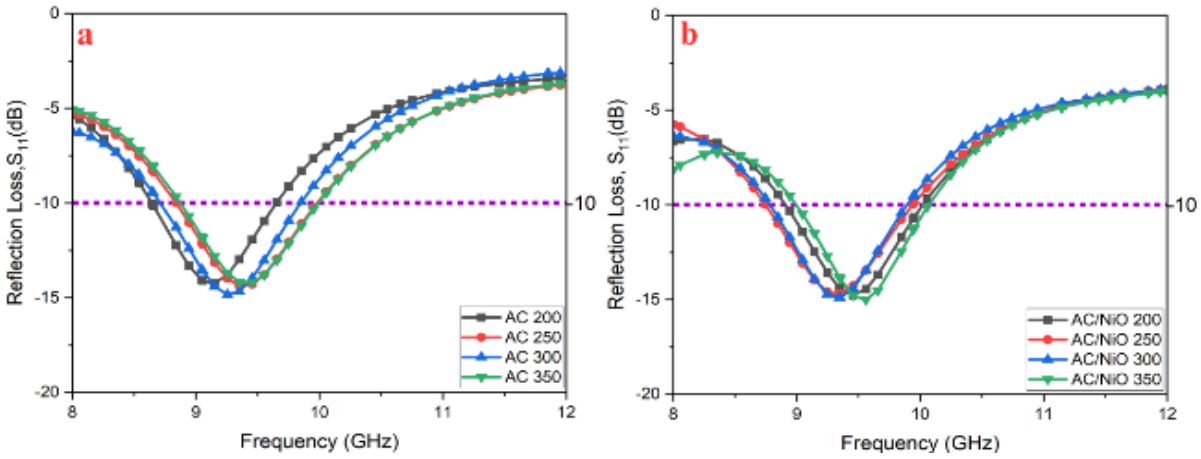

Figure 5. Reflection loss of (a) AC, and (b) AC/NiO at different temperatures carbonization.

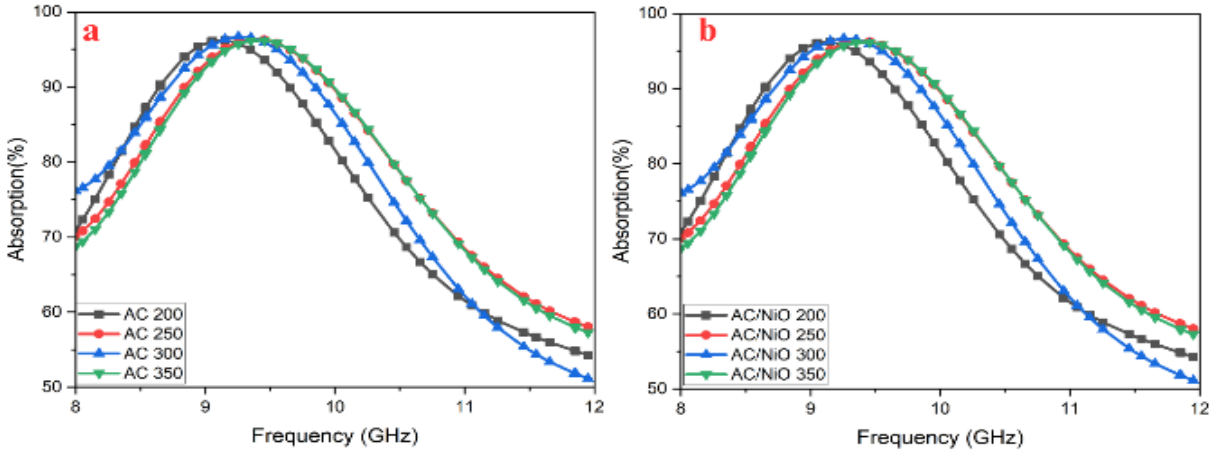

Figure 6. Absorption of (a) AC, and (b) AC/NiO at different temperatures carbonization.

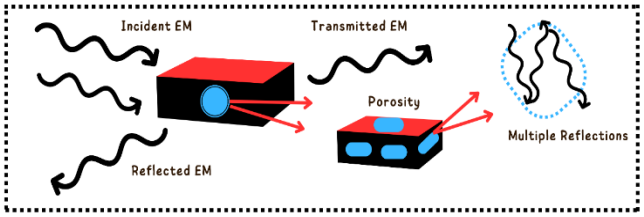

Figure 7. MW Absorption Mechanisms.

Absorption of (a) AC and (b) AC/NiO at different temperatures carbonization were derived using Equation (4). The resonant frequency of AC samples rose at higher carbonization temperatures, leading to a more graphitized structure with enhanced conductivity and dielectric characteristics. This transition resulted in enhanced absorption efficiency, with peak absorption rates at various temperatures nearing 96.2% to 96.7% as shown in Figure 6. The incorporation of NiO into AC/NiO improved microwave absorption by leveraging the dielectric loss from AC and the magnetic loss from NiO. Nonetheless, the overall absorption efficiency does not markedly surpass that of pure AC. Both materials exhibit exceptional absorption (>96%), although AC/NiO provides a wider absorption bandwidth owing to the synergistic interplay of magnetic and dielectric losses. For ideal microwave absorbers, achieving at least 90% absorption [31-33] is necessary to ensure that the incoming electromagnetic signal is effectively absorbed and not transmitted or reflected (Figure 7.).

To evaluate the microwave absorption performance of our AC and AC/NiO composites, we compared our results with similar biomass-derived materials reported in the literature. For example, Yang *et al.* [5] documented a ZnO loaded porous carbon composite derived from banana peels, which achieved a minimum reflection loss (RL) of –42.1 dB at 10.4 GHz with a thickness of 3 mm. Similarly, Che *et al.* [34] reported a maximum RL of –30.5 dB and an effective absorption bandwidth (EAB) of 3.8 GHz using bimetallic sulfides embedded in biomass-derived porous carbon. In contrast, our highest-performing AC/NiO 350 composite shows an RL of –15.03 dB at 9.54 GHz and an EAB of approximately 1.6 GHz at a thickness of 6 mm. While our RL value is lower than that of some metal-based composites, the advantages of our synthesis method which is its simplicity, eco-friendliness, and high absorption efficiency of over 96%, demonstrate its practicality for sustainable absorber applications. Compared to coconut shell-derived carbon activated with KOH, which reported an RL of –48.87 dB at 8.7 GHz [35], our method utilizes less corrosive activation with HCl, achieving adequate performance while minimizing processing hazards. These comparisons highlight the competitive potential of our AC/NiO composites as effective and environmentally friendly alternatives for microwave absorbers.

4. Conclusions

The MW absorption of coconut fiber samples was studied. The sample was prepared via chemical activation with HCI and carbonized at four different temperatures: 200°C, 250°C, 300°C, and 350°C, respectively. AC and AC/NiO materials exhibit exceptional absorption of more than 96%). However, AC/NiO carbonized at 350°C showed excellent MW absorption performance with a RL_{min} value of −15.03 dB at 9.54 GHz with an optimum thickness at 6.0 mm. The good absorption performance of AC/NiO at 350°C can be attributed to good conduction loss and interfacial polarization. The numerous numbers of pores also induce multiple reflections of MW through high conductivity. Therefore, it can conclude that AC from coconut fibre sample can be a good candidate for effective absorption of EM wave at X-band frequency. It has also been concluded that the need for AC and nickel oxide needs to increase as an improvement of an absorption wave.

Acknowledgements

This work funded under Ministry of Higher Education Malaysia for Fundamental Research Grant Scheme with Project Code: FRGS/1/2020/TK0/USM/02/31 and partially supported by the Asia-Africa Core-to-Core program provided Japan Society for Promotion of Science (Project No. JPJSCCB20240005).

References

[1] X. Xiong, H. Zhang, H. Lv, L. Yang, G. Liang, J. Zhang, Y. Lai, H-W. Cheng, and R. Che, "Recent progress in carbon-based materials and loss mechanisms for electromagnetic wave absorption," *Carbon,* vol. 219, p. 118834, 2024.

[2] Z. Duan, Y. Zhang, T. Yang, Z. Lv, Y. Bai, D. Liu, and T. Peng, "Constructing core-shell biomass carbon@Fe_3O_4 composites for enhanced mid-to-low frequency electromagnetic wave absorption," *Materials Research Bulletin*, vol. 177, p. 112853, 2024.

[3] C. Liu, M. Han, J. Lin, W. Liu, J. Liu, and Z. Zeng, "Wood biomass-derived carbon for high-performance electromagnetic wave absorbing and shielding," *Carbon*, vol. 208, pp. 255–276, 2023.

[4] E. C. Gokce, M. D. Calisir, S. Selcuk, M. Gungor, and M. E. Acma, "Electromagnetic interference shielding using biomass-derived carbon materials," *Materials Chemistry and Physics*, vol. 317, p. 129165, 2024.

[5] X. Yang, W. Ye, Y. Zhang, Z. Chen, Z. Zhou, K. Gao, W. Xue, and R. Zhao, "In situ loading of ZnO on hierarchical porous carbon derived from banana-peel waste to enrich mechanism for microwave absorption," *Journal of Alloys and Compounds*, vol. 1003, p. 175522, 2024.

[6] J. Zhang, L. Zhang, C. Lv, L. Gao, C. Xueqi, S. Luo, Y. Chen, Y. Ren, L. Chang, W. Guo, and Q. Tang, "Lightweight, ultra-strength, multifunctional MXene/wood composite film designed by densification strategy for electrode, thermal management, and electromagnetic shielding application," *Industrial Crops and Products*, vol. 216, p. 118700, 2024.

[7] Z.-X. Wang, X.-S. Han, Z.-J. Zhou, W.-Y. Meng, X-W. Han, S-J. Wang, and J-W. Pu, "Lightweight and elastic wood-derived composites for pressure sensing and electromagnetic interference shielding," *Composites Science and Technology*, vol. 213, p. 108931, 2021.

[8] J. Che, H. Zheng, Z. Lu, Z. Yang, Y. Gao, and Y. Wang, "Bimetallic sulfides embedded into porous carbon composites with tunable magneto-dielectric properties for lightweight biomass-reinforced microwave absorber," *Ceramics International*, vol. 49, no. 16, pp. 27094–27106, 2023.

[9] N. Wang, K. Nan, H. Zheng, Q. Xue, W. Wang, and Y. Wang, "Two-phase magnetic nanospheres with magnetic coupling effect encapsulated in porous carbon to achieve lightweight and efficient microwave absorbers," *Journal of Colloid and Interface Science*, vol. 671, pp. 56–66, 2024.

[10] Y. Cheng, M. Chen, K. Xia, H. Li, G. Xu, L. Yang, Z. Zhao, P. Liu, and L. Wang, "Rapid conversion of biomass to hierarchical porous carbons via one-step microwave carbonization/activation for long cycle-stable supercapacitor and zinc-ion capacitor," *Journal of Power Sources*, vol. 624, p. 235523, 2024.

[11] Anjana, and A. Chandra, "Facile synthesis and characterization of polymer composites with cobalt ferrite and biomass based activated carbon for microwave absorption," *Materials Today Communications*, vol. 37, p. 107397, 2023.

[12] M. Wang, H. Pan, L. Xu, Y. Teng, X. Fu, Y. Zhang, M. Dou, Z. Liu, X. Huang, L. Hu, and Y. Wang, "Microwave-absorbed porous carbon was prepared from agricultural coconut shell waste by a simple one-step high temperature charring," *Materials Science and Engineering: B*, vol. 307, p. 117509, 2024.

[13] G. J. H. Melvin, Z. Wang, Q. Q. Ni, N. J. Siambun, and M. M. Rahman, "Electromagnetic wave absorption properties of rice husks carbonized at 2500°C," *AIP Conference Proceedings*, vol. 1091, no. 1, p. 020002, 2017.

[14] Z. Zulpadrianto, Y. Yohandri, and A. Putra, "Development radar absorber material using rice husk carbon for anechoic chamber application," *IOP Conference Series: Materials Science and Engineering*, vol. 335, no. 1, p. 012002, 2018.

[15] H. Soleimani, J. Y. Yusuf, H. Soleimani, L. K. Chuan, and M. Sabet, "Banana-peel derived activated carbon for microwave absorption at X-band frequency," *Synthesis and Sintering*, vol. 2, no. 3, pp. 120–124, 2022.

[16] C. Wang, J. Li, and S. Guo, "High-performance electro-magnetic wave absorption by designing the multilayer graphene/thermoplastic polyurethane porous composites with gradient foam ratio structure," *Composites Part A: Applied Science and Manufacturing*, vol. 125, p. 105522, 2019.

[17] Z. Wu, K. Tian, T. Huang, W. Hu, F. Xie, J. Wang, M. Su, and L. Li, "Hierarchically porous carbons derived from biomasses with excellent microwave absorption performance," *ACS Applied Materials & Interfaces*, vol. 10, no. 13, pp. 11108–11115, 2018.

[18] Y. Cheng, Z. Li, Y. Li, S. Dai, G. Ji, H. Zhao, J. Cao, and Y. Du, "Rationally regulating complex dielectric parameters of meso-porous carbon hollow spheres to carry out efficient microwave absorption," *Carbon*, vol. 127, pp. 643–652, 2018.

[19] W. Yang, L. Li, Y. Hou, Y. Liu, and X. Xiao, "Enhanced electromagnetic wave absorption of SiOC/porous carbon composites," *Materials*, vol. 15, no. 24, 2022.

[20] B. D. Zdravkov, J. J. Čermák, M. Šefara, and J. Janků, "Pore classification in the characterization of porous materials: A perspective," *Central European Journal of Chemistry*, vol. 5, no. 2, pp. 385–395, 2007.

[21] J. Y. Yusuf, H. Soleimani, N. Yahya, Y. K. Sanusi, G. Kozlowski, A. Ochsner, L. L. Adebayo, F. A. Wahaab, S. Sikiru, and B. B. Balogun, "Electromagnetic wave absorption of coconut fiber-derived porous activated carbon," *Boletin de la Sociedad Espanola de Ceramica y Vidrio*, vol. 61, no. 2, pp. 417–427, 2022.

[22] Q. Chen, X. Liu, T. Wang, X. Su, M. Liu, S. Chaemchuen, and F. Verpoort, "A solvent-free process enabling ZnO/porous carbon with enhanced microwave absorption," *Journal of Materials Science & Technology*, vol. 149, pp. 255–264, 2023.

[23] J. Chen, G. Song, Z. Liu, L. Xie, S. Zhang, and C. Chen, "Design of core-shell nickel oxide/silicon carbide whiskers towards excellent microwave absorption property," *Chinese Journal of Chemical Engineering*, vol. 37, pp. 208–216, 2021.

[24] C. Ni, D. Wu, X. Xie, B. Wang, H. Wei, Y. Zhang, X. Zhao, L. Liu, B. Wang, and W. Du, "Microwave absorption properties of microporous CoNi@(NiO-CoO) nanoparticles through dealloying," *Journal of Magnetism and Magnetic Materials*, vol. 503, p. 166631, 2020.

[25] S. G. Danjumma, Y. Abubakar, and S. Suleiman, "Nickel oxide (NiO) devices and applications: A review," *International Journal of Engineering Research & Technology (IJERT)*, vol. 08, no. 04, 2019.

[26] O. Luukkonen, S. I. Maslovski, and S. A. Tretyakov, "A stepwise Nicolson-Ross-Weir-based material parameter extraction method," *IEEE Antennas and Wireless Propagation Letters*, vol. 10, pp. 1295–1298, 2011.

[27] S. Zva, and S. Znb, "Measurement of dielectric material properties application note products," Rohde & Schwarz Benelux B.V. 2012

[28] L. S. Rocha, C. C. Junqueira, E. Gambin, A. N. Vicente, A. E. Culhaoglu, and E. Kemptner, "A free space measurement approach for dielectric material characterization," in *SBMO/IEEE MTT-S International Microwave and Optoelectronics Conference Proceedings*, 2013.

[29] Z. Liu, Y. Wang, C. Xian, K. Li, F. Wang, P. Zhang, W. Yang, S. Liu, C. Wang, H. Du, Z. Luo, J. Tang, X. Kong, L. Han, Y. Hou, and J. Yang, "High-performance microwave absorbers using a simple double-layer absorbing structure to improve impedance mismatching," *Journal of Alloys and Compounds*, vol. 938, p. 168649, 2023.

[30] W. You, and R. Che, "Excellent NiO-Ni nanoplate microwave absorber via pinning effect of antiferromagnetic-ferromagnetic interface," *ACS Applied Materials & Interfaces*, vol. 10, no. 17, pp. 15104–15111, 2018.

[31] Q. V. Thi, S. Park, J. Jeong, H. Lee, J. Hong, C. M. Koo, N. T. Tung, and D. Sohn, "A nanostructure of reduced graphene oxide and NiO/ZnO hollow spheres toward attenuation of electromagnetic waves," *Materials Chemistry and Physics*, vol. 266, p. 124530, 2021.

[32] A. S. Shamshirgar, M. F. Alvarez, A. d. Campo, J. F. Fernandez, R. E. R. Hernandez, R. Ivanov, J. Rosen, and I. Hussainova, "Versatile graphene-alumina nanofibers for microwave absorption and EMI shielding," *Carbon*, vol. 210, p. 118057, 2023.

[33] K. Al-Badri, "Design of a perfect metamaterial absorber for microwave applications," *Basic and Applied Sciences - Scientific Journal of King Faisal University*, vol. 22, no. 1, pp. 144–147, 2021

[34] S. Chakraborty, and S. Chakraborty, "A review on the pursuit of an optimal microwave absorber," *Facta universitatis - series: Electronics and Energetics*, vol. 34, no. 4, pp. 631–645, 2021.

[35] H. Soleimani, J. Y. Yusuf, N. Yahya, A. R. Sadrolhosseini, M. Sabet, and L. A. Lanre, "Microwave absorption of coconut wasted derived activated carbon," *Fundamental and Applied Sciences, ICFAS 2020*, 2021.